Physiol Genomics 43: 110–120, 2011.
First published November 16, 2010; doi:10.1152/physiolgenomics.00115.2010.

CALL FOR PAPERS | *Technology Development for Physiological Genomics*

A gene expression signature for insulin resistance

Nicky Konstantopoulos,[1]* Victoria C. Foletta,[1]* David H. Segal,[1] Katherine A. Shields,[2] Andrew Sanigorski,[1] Kelly Windmill,[1] Courtney Swinton,[1] Tim Connor,[1] Stephen Wanyonyi,[1] Thomas D. Dyer,[3] Richard P. Fahey,[1] Rose A. Watt,[1] Joanne E. Curran,[3] Juan-Carlos Molero,[1] Guy Krippner,[4] Greg R. Collier,[5] David E. James,[6] John Blangero,[3] Jeremy B. Jowett,[2] and Ken R. Walder[1,7]

[1]*Metabolic Research Unit, School of Medicine, Deakin University, Geelong and* [2]*Baker IDI Heart and Diabetes Institute, Melbourne, Australia;* [3]*Southwest Foundation for Biomedical Research, San Antonio, Texas; and* [4]*Verva Pharmaceuticals and* [5]*ChemGenex Pharmaceuticals, Geelong;* [6]*Diabetes and Obesity Research Program, Garvan Institute, Sydney; and* [7]*Institute of Technology and Research Innovation, Deakin University, Geelong, Australia*

Submitted 8 June 2010; accepted in final form 8 November 2010

Konstantopoulos N, Foletta VC, Segal DH, Shields KA, Sanigorski A, Windmill K, Swinton C, Connor T, Wanyonyi S, Dyer TD, Fahey RP, Watt RA, Curran JE, Molero JC, Krippner G, Collier GR, James DE, Blangero J, Jowett JB, Walder KR. A gene expression signature for insulin resistance. *Physiol Genomics* 43: 110–120, 2011. First published November 16, 2010; doi:10.1152/physiolgenomics.00115.2010.—Insulin resistance is a heterogeneous disorder caused by a range of genetic and environmental factors, and we hypothesize that its etiology varies considerably between individuals. This heterogeneity provides significant challenges to the development of effective therapeutic regimes for long-term management of type 2 diabetes. We describe a novel strategy, using large-scale gene expression profiling, to develop a gene expression signature (GES) that reflects the overall state of insulin resistance in cells and patients. The GES was developed from 3T3-L1 adipocytes that were made "insulin resistant" by treatment with tumor necrosis factor-α (TNF-α) and then reversed with aspirin and troglitazone ("resensitized"). The GES consisted of five genes whose expression levels best discriminated between the insulin-resistant and insulin-resensitized states. We then used this GES to screen a compound library for agents that affected the GES genes in 3T3-L1 adipocytes in a way that most closely resembled the changes seen when insulin resistance was successfully reversed with aspirin and troglitazone. This screen identified both known and new insulin-sensitizing compounds including nonsteroidal anti-inflammatory agents, β-adrenergic antagonists, β-lactams, and sodium channel blockers. We tested the biological relevance of this GES in participants in the San Antonio Family Heart Study (n = 1,240) and showed that patients with the lowest GES scores were more insulin resistant (according to HOMA_IR and fasting plasma insulin levels; $P < 0.001$). These findings show that GES technology can be used for both the discovery of insulin-sensitizing compounds and the characterization of patients into subtypes of insulin resistance according to GES scores, opening the possibility of developing a personalized medicine approach to type 2 diabetes.

microarray; screening; diabetes; personalized medicine

GENE EXPRESSION SIGNATURES (GESs) were first described as clusters of coordinately expressed genes (2) and were further defined as the expression pattern of a small set of genes that consistently and robustly represent the integrated biological response of a cell or tissue to its environment without necessarily incorporating genes playing a direct role in the changed metabolic state (47). GESs have been used in oncology to assist in tumor classification, prognosis, and patient response to therapies (11, 32). The application of GESs in oncology has also been extended to smaller gene subsets for use in compound library screening to search for small molecules that induce gene expression patterns with high similarity to the GES (41, 42). We sought to extend the GES approach to the field of insulin resistance and type 2 diabetes.

Type 2 diabetes is a major health issue worldwide, and a key feature of this disease is insulin resistance. The causes of insulin resistance are multifactorial and can include elevated circulating levels of nonesterified fatty acids and inflammatory cytokines, endoplasmic reticulum stress, and oxidative stress (reviewed in Ref. 29). We hypothesized that a GES that reflects the insulin sensitivity of a cell could be identified and subsequently used to screen a compound library for insulin-sensitizing agents. To test this hypothesis, we developed an in vitro model system to mirror the amelioration of insulin resistance by therapeutics that is known to reverse the impaired glucose tolerance associated with type 2 diabetes.

In this model, 3T3-L1 adipocytes were rendered either "insulin resistant" by treatment with the proinflammatory cytokine tumor necrosis factor-α (TNF-α) or "insulin resensitized" by treatment first with TNF-α and second with established insulin sensitizers aspirin (acetylsalicylic acid, ASA) and troglitazone (TGZ) (27, 51) to reverse the effects of TNF-α (Fig. 1*A*). Insulin sensitivity was assessed by 2-deoxyglucose (2-DOG) uptake as the functional end point. We then performed large-scale gene expression profiling and Bayesian model selection to identify a GES consisting of a small subset of genes whose expression patterns most robustly and significantly represented the difference between the insulin-resistant and insulin-resensitized states in TNF-α-treated 3T3-L1 adipocytes. Our study provides evidence that an in vitro-derived GES stratified a human population according to their level of insulin resistance, and that it can be used to screen a small compound library to search for new insulin-sensitizing compounds.

* N. Konstantopoulos and V. C. Foletta contributed equally to this work.

Address for reprint requests and other correspondence: N. Konstantopoulos, Metabolic Research Unit, Deakin Univ., Waurn Ponds, VIC 3217, Australia (e-mail: nicky.konstantopoulos@deakin.edu.au).

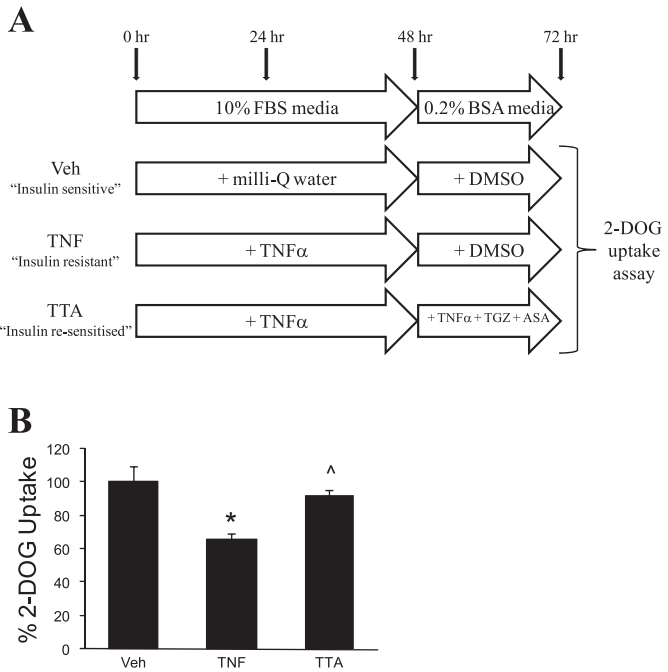

Fig. 1. Reversal of tumor necrosis factor-α (TNF-α)-induced insulin resistance in 3T3-L1 adipocytes. *A*: 3T3-L1 adipocytes were treated for 72 h with vehicle (Veh), 3 ng/ml TNF-α (TNF), or TNF-α + 10 μM troglitazone (TGZ) and 5 mM aspirin (acetylsalicylic acid, ASA), with ASA and TGZ only added in the final 24 h (TTA). Cells were then treated with insulin (0 or 10 nM) for 30 min, followed by measurement of 2-deoxyglucose (2-DOG) uptake over the final 10 min of insulin stimulation. *B*: data are presented as % change in insulin-stimulated 2-DOG uptake compared with vehicle-treated, insulin-stimulated cells and represent means ± SE of 6 independent experiments; each data point was assayed in triplicate. The fold increase in 2-DOG uptake in vehicle-treated, insulin-stimulated adipocytes was 6.6 ± 0.6 above basal level ($P < 0.001$ compared with vehicle-treated alone). The average amount of 2-DOG transported in vehicle-treated adipocytes was 20.5 ± 3.4 pmol·min^{-1}·well^{-1}. *$P < 0.001$ compared with Veh; ^$P < 0.001$ compared with TNF. Statistical analyses were performed with 1-way ANOVA, and multiple testing correction was performed with Tukey honestly significant difference (HSD).

EXPERIMENTAL PROCEDURES

Cell Culture and Treatments

3T3-L1 fibroblasts were cultured and differentiated as described previously (20). Adipocytes were used for experiments 7–12 days after the initiation of differentiation, at which time >80% of fibroblasts had differentiated into mature adipocytes. As illustrated in Fig. 1*A*, differentiated 3T3-L1 adipocytes were treated with vehicle (milli-Q water) or 3 ng/ml TNF-α (Peprotech, Rocky Hill, NJ) for 48 h in Dulbecco's modified Eagle's medium (DMEM; GIBCO Invitrogen, Melbourne, Australia) containing 10% (vol/vol) heat-inactivated FBS (Invitrogen). Adipocytes were then treated for a further 24 h with 0.1% DMSO (vehicle), 3 ng/ml TNF-α and 0.1% DMSO ("insulin resistant"), or 3 ng/ml TNF-α, 5 mM ASA (Sigma-Aldrich, Sydney, Australia), and 10 μM TGZ (Sigma-Aldrich) ("insulin resensitized") in serum-free DMEM containing 0.2% (wt/vol) RIA-grade BSA (Sigma-Aldrich). Treatments were replenished every 24 h.

2-Deoxyglucose Uptake

Glucose transport was measured as 2-deoxy-[U-^{3}H]glucose uptake as described elsewhere (20). Briefly, treated 3T3-L1 adipocytes in 24-well plates were washed twice in Dulbecco's PBS, pH 7.4 (GIBCO Invitrogen) containing 0.2% (wt/vol) RIA-grade BSA, 0.5 mM $MgCl_2$, and 0.9 mM $CaCl_2$. Insulin (Humulin R; Novo Nordisk, Baulkham Hills, Australia) at 0 and 10 nM was added for 30 min at 37°C. Uptake of 50 μM 2-DOG and 0.5 μCi 2-deoxy-[U-^{3}H]glucose (NEN, PerkinElmer Life Sciences, Melbourne, Australia) per well was measured over the final 10 min of insulin stimulation. The reaction was stopped by addition of 80 μg/ml ice-cold phloretin (Sigma-Aldrich) in PBS, and cells were then solubilized in 0.03% (wt/vol) SDS (GIBCO Invitrogen). Counts per minute were measured by a 2900TR-LSA scintillation counter (Packard Bioscience, PerkinElmer Life Sciences). Data were analyzed with Statistical Package for the Social Sciences software (SPSS version 17.0; Fullerton, CA). Analyses were performed on data where normality of distribution was considered with the Kolmogorov-Smirnov test. Data were analyzed with one-way ANOVA analysis with post hoc Tukey honestly significant difference (HSD), and the mean difference was considered significant at the 0.05 level.

Generation of GES

RNA extractions and microarrays. Unannotated mouse skeletal muscle cDNA microarrays containing ~12,000 elements (with a redundancy rate of 21%) were generated and hybridized as described previously (9). Total RNA was extracted from 3T3-L1 adipocytes treated with vehicle (0.1% DMSO, $n = 20$), TNF-α ($n = 20$), or TNF-α plus ASA and TGZ ($n = 20$) with TRIzol reagent and purified with RNA cleanup columns as per manufacturer's instructions (Invitrogen). The quality and quantity of the RNA were determined with the Agilent Bioanalyzer and RNA 600 Nano Assay kit (Agilent, Melbourne, Australia). Fluorescence-labeled cDNA was prepared from 20 μg of total RNA with indirect labeling and hybridized to the microarray slides. An identical reference RNA, prepared from pooled experimental RNA, was used across all hybridizations. For all hybridizations, cDNA from the reference RNA was labeled with Cy3, while experimental cDNA was labeled with Cy5. Fluorescent images of the microarrays were acquired with a 4000B scanner, and data were extracted with GenePix Pro 5.1 software (Molecular Devices, Melbourne, Australia). Normalization and primary microarray data analysis were performed with Acuity 4 software (Molecular Devices) as detailed previously (9). The microarray data set generated from this study conforms to the MIAME guidelines and is available at Gene Expression Omnibus (GEO; **http://www.ncbi.nlm.nih.gov/geo/query/acc.cgi**) series record GSE18103.

Selection of GES. Two statistical approaches were compared and used to identify the optimal set of genes (GES) that best predicts the reversal of the insulin resistance state (TNF-α + TGZ and ASA treatment group) from the insulin resistance state (TNF-α-alone treatment group). Given a set of 20 replicates per treatment, the predictive set of genes was limited to <8 in order to guarantee sufficient statistical estimation of joint predictors. A GES of up to eight genes was also preferred in view of its subsequent requirement—a manageable number of genes that can be multiplexed and measured for screening a compound library.

The first approach used a combination of diagonal linear discriminant analysis (DLDA) and the signal-to-noise ratio (SNR) statistic as described by Stegmaier et al. (41). To select the genes that were significantly different between vehicle and TNF-α-alone treatment groups ($P < 0.01$), pairwise comparisons between the two treatment groups by Student's *t*-test were performed. With only the set of genes that were affected by the TNF-α treatment, DLDA was then performed to identify the genes that best discriminate the TNF-α-alone treatment group from the TNF-α plus TGZ and ASA treatment group. Briefly, the DLDA algorithm (using Acuity software) classified the TNF-α-alone-treated microarray data set as one group and the TNF-α plus TGZ and ASA-treated microarray data set as another group. With a forward stepwise variable selection, DLDA identified the minimal set of genes with optimal ability to separate each data set into the two groups specified, in our case, the TNF-α-alone-treated group versus the TNF-α plus TGZ and ASA-treated group. The SNR statistic was used to rank the DLDA-selected genes according to their discriminat-

ing ability. SPSS was then used to reduce signature genes to a small subset that were discriminating and displayed divergent expression profiles.

The second approach used Bayesian methods, which allow greater flexibility to thoroughly model all of the available information and thus model all possible gene combinations (7). A preliminary analysis of the microarray data was performed with a robust linear model (based on a multivariate *t* distribution) with accompanying likelihood ratio test to identify each transcript that showed at least a suggestive nominal difference in expression between the insulin-resistant and insulin-resensitized treatment groups ($P < 0.01$). A Bayesian model selection procedure was next employed (7) in which all possible models of up to eight genes were generated to obtain a Bayesian-averaged regression equation that served as the GES. The models were then examined for their ability to differentiate accurately between the treatment groups by direct testing using an objective Bayesian selection mechanism. The selection was then refined with an additional weighting (truncated Poisson distribution) that favors models of lower complexity, that is, with fewer contributing genes in the GES.

The first approach identified one GES that exhibited the best statistical ability to discriminate between the treatment groups. The Bayesian approach identified 20 GESs (including the GES from the first approach) and ranked them according to their predictive power. The total number of genes that were identified in the 20 putative GES sets with both statistical approaches was only 20, indicating the considerable redundancy in the genes included in the various GES gene sets. Each gene was then sequenced and validated (detailed below), and the gene set with the expression profile validated in all technologies used [from microarray to real-time PCR and matrix-assisted laser desorption/ionization (MALDI)-time of flight (TOF)-based quantitative analysis system] was selected. The result of these analyses was the identification of a GES of five genes that fulfilled the following criteria: *1*) gene expression profile was validated by other technologies and in other samples; *2*) the validated set of genes retained the best predictive power to discriminate the insulin-resistant treatment group from the insulin-resensitized treatment group; and *3*) since the GES needed to be relevant beyond the cell culture model that it was derived from (to identify novel insulin-sensitizing agents), the GES genes must also be expressed in human lymphocytes (detailed below).

Gene validation. The unknown cDNAs representing the GES were identified by sequencing using an ABI 1300 genetic analyzer. To confirm the gene expression profile exhibited by the microarray, gene expression was analyzed by semiquantitative real-time PCR (qPCR) using Brilliant SYBR Master Mix (Stratagene, La Jolla, CA) on the MX3005P QPCR system (Stratagene). Validation was performed on the same RNA/cDNA used for microarray (technical replication) as well as alternative sets of treated samples (biological replication). The qPCR conditions were 95°C for 10 min and 40 cycles of 95°C for 30 s and 60°C for 1 min. Relative gene expression was calculated as $2^{-\Delta C_t}$, where C_t is threshold cycle. The expression levels of the housekeeping gene cyclophilin were not altered with any of the treatments (data not shown). Table 1 displays the list of primer sequences. Data were tested for normality of distribution by the Kolmogorov-Smirnov test with SPSS. Data were analyzed by one-way ANOVA with post hoc Tukey HSD to adjust *P* values for multiple comparison. $P < 0.05$ was considered statistically significant.

Compound Library Screen

3T3-L1 adipocytes at *day 7* after differentiation in gelatin-coated 96-well plates were treated with TNF-α (3 ng/ml, 48 h, 37°C) in DMEM containing 10% FBS and then treated for a further 24 h with 3 ng/ml TNF-α and 10 μM compound in serum-free DMEM containing 0.2% BSA. Compounds were obtained from a chemical library consisting of 1,120 agents including off-patent drugs, bioactive alkaloids, and proprietary natural products. Vehicle (0.1% DMSO; $n = 4$)-, TNF-α ($n = 4$)-, and TNF-α plus ASA and TGZ ($n = 2$)-treated wells serving as controls were included on each assay plate to obtain a confidence interval, and treatments were replenished every 24 h. All plates where controls did not fall within 2 standard deviations of the mean for all plates were rejected. RNA was extracted from each well with RNeasy 96 Kits (Qiagen, Melbourne, Australia), and gene expression levels of the five GES genes were multiplexed and quantified with the MALDI-TOF-based quantitative gene expression analysis system (MassARRAY; Sequenom, San Diego, CA) (12).

To score the results of the screen, a custom algorithm was developed to allow the measurements of each of the five GES genes to be combined to provide a single score (termed "GES score" throughout). The gene expression levels of routinely used housekeeping genes [aldo-keto reductase family 1, member A4 (AKR1A4), NCBI accession no. NM_021473; peptidylprolyl isomerase A (PPIA/cyclophilin A), NCBI accession no. NM_008907] were not constant across the experimental groups (data not shown). Therefore, to control for the different amounts of input cDNA, the raw expression levels of each measured gene were summed to give a total expression value. Each gene's expression level was then expressed relative to this total expression value, which was performed by taking the residual following a regression between the gene and the sample's total expression value. In independent tests, we observed that this most closely matched input cDNA amounts as measured by spectrophotometric means across treatments (data not shown). The resulting distribution across all treatments was standardized (*z* score) in order to allow direct comparison across all genes and between samples. This is referred to as the "normalized expression level of the gene."

To generate the final score for each treatment, an algorithm derived from the optimal statistical model for discriminating between the insulin-resistant and insulin-resensitized states were used. The β-correlation coefficient from the model was applied to each of the five genes to account for the relative contribution that each gene made to the predictive power of the total GES. Correlation coefficients were used to multiply the measured gene expression level and summed to

Table 1. *Primer sequences for qPCR analyses of the 5 genes comprising the TNF-α-based GES and the housekeeping gene*

Gene Name	NCBI Reference No.	Forward Primer	Reverse Primer
ACS1	NM_007981	tggtcgtcccgctctatga	tcacagagagttcagctttgttcac
CD63	NM_007653	agtgtgtcaagtttttgctctacgtt	caccaatggcgatcaatcc
STEAP4	NM_054098	ccagtcaggaacactagatgcaa	agcccaagagtacgagcaatg
Skp1a	NM_011543	gggaccaagaattcctgaaagtt	gcatgtgacatcaagcaaacct
PKM2	NM_011099	caagatcatcagcaaatcgagaa	cccatcactggcctccaa
Ppia	*NM_008907*	*cccaccgtgttcttcgaca*	*ccagtgctcagagctcgaaa*

qPCR, quantitative real-time PCR; TNF-α, tumor necrosis factor-α; GES, gene expression signature; ACSl, acyl-CoA synthetase long-chain family member 1/FACL2, fatty acid-coenzyme A ligase, long-chain 2; STEAP4, six transmembrane epithelial antigen of the prostate/TIARP, TNF-α-induced adipose-related protein/STAMP2, six transmembrane protein of prostate 2; Skp1a, S-phase kinase associated protein 1A; PKM2, pyruvate kinase, muscle 2; Ppia, peptidylprolyl isomerase A/cyclophilin A. Italics, data not shown.

give a single metric. The resulting custom algorithm was ([+]0.706 × ACS1) + ([−]0.646 × CD63) + ([−]0.825 × Skp1a) + ([−]0.502 × PKM2) + ([−]0.594 × STEAP4). In the example of ACS1, 0.706 is the β-correlation coefficient for the gene, [+] indicates the direction of change from TNF-α to TNF-α plus ASA and TGZ treatment groups, and the ACS1 term denotes the value of the normalized expression level of the gene. A positive final score indicates a compound that may be more similar to the vehicle (insulin sensitive) and/or TNF-α plus ASA and TGZ (insulin resensitized) treatment groups, and a negative final score denotes a compound acting more like the TNF-α (insulin resistant) treatment group. The compounds were ranked by this GES score. Data were analyzed with SPSS. The Kruskal-Wallis nonparametric test was used to determine which compound families had mean GES scores that were statistically different from the TNF-α and TNF-α plus ASA and TGZ treatment groups. *P* values were adjusted for multiple comparison testing with the Bonferroni correction. $P < 0.05$ was considered significant.

Intact Cell GLUT4 Translocation Assay

3T3-L1 fibroblasts were infected at 50% confluence with retrovirus from Plat-E packaging cells transfected with hemagglutinin (HA)-tagged GLUT4 in the replication-incompetent retroviral vector pBABE puro as detailed previously (15). Puromycin (2 μg/ml) selection was placed on cells 48 h after infection, and cells were induced to differentiate as described above. Forty-eight hours before the translocation assay, adipocytes were seeded into gelatin-coated black-wall clear-bottom 96-well plates (BD Biosciences, North Ryde, Australia), and then 24 h before the assay cells were treated with each compound at 10 μM in serum-free DMEM containing 0.2% (wt/vol) RIA-grade BSA. On the day of the translocation assay, cells were incubated in the absence or presence of insulin (0.5 or 200 nM) in DMEM (serum- and bicarbonate free) containing 0.2% RIA-grade BSA and 0.02 M HEPES, pH 7.4 for 20 min at 37°C. The percentage of HA-tagged GLUT4 at the cell surface was measured and calculated as previously described (15, 20). Data were tested for normality of distribution with the Kolmogorov-Smirnov test and analyzed with unpaired Student's *t*-test with two-tailed distribution. Data were considered significant at $P < 0.05$.

Human Study

Gene expression profiles were generated on lymphocyte samples from participants in the San Antonio Family Heart Study (SAFHS), which investigates the genetics of cardiovascular disease in Mexican Americans (28). Peripheral blood samples, with subsequent lymphocyte preparation, were obtained in the morning after an overnight fast. High-quality RNA was obtained from 1,240 individuals. Most of these individuals (89%) are members of 30 extended families, with 10–87 phenotyped individuals spanning up to 4 generations of each family. Individual families were ascertained through a single adult proband from the Mexican American community, independent of phenotype. The sample contains 506 men (40.8%) and 734 women (59.2%) with a mean age of 39.3 yr (ranging from 15 to 94 yr). This data set includes anthropometric measurements [such as body mass index (BMI)], insulin sensitivity measures (oral glucose tolerance test), and standard blood chemistry parameters including levels of plasma glucose, insulin, and lipids. The Institutional Review Board of the University of Texas Health Science Center at San Antonio approved all procedures and research. Informed written consent was obtained from each participant, and the study conforms to the standards outlined by the Declaration of Helsinki. Analyses of the samples from the SAFHS were approved by the Deakin University Human Research Ethics Committee in accordance with the National Health and Medical Research Council of Australia (NH&MRC) National Statement on Ethical Conduct in Human Research.

Lymphocyte profiling and statistical analyses. Genomewide transcriptional profiles were generated with Illumina Sentrix Human Whole Genome (WG-6) Series I BeadChips and the Illumina BeadArray 500GX Reader (14). The identification of expressed transcripts and the standardization steps that were used to make the expression values comparable across individuals and across transcripts have been described in detail elsewhere (14). The raw and normalized gene expression values of all 19,648 analyzed transcripts are available under accession number E-TABM-305. To represent each individual's GES score, the same formula as above was used to determine the standardized expression values of each of the five GES genes as a single score. Using the information collected in the SAFHS, we then looked for a relationship between individuals' GES scores with fasting insulin and glucose levels and HOMA_IR (homeostasis model of assessment for insulin resistance based on insulin and glucose) using Pearson's correlation. All statistical analyses were carried out with SPSS, and *P* values were corrected for multiple comparison with a conservative Bonferroni correction. Correlation was considered significant at the 0.01 level (2 tailed).

RESULTS

Identification of a Five-Gene GES That Discriminates Between Insulin-Resistant and Insulin-Resensitized States

The use of the cell model allowed us to define the cause of insulin resistance (inflammation based) in this typically multifactorial pathology in individuals. After exposure of 3T3-L1 adipocytes to 3 ng/ml TNF-α for 72 h, insulin-stimulated 2-DOG uptake was reduced by 35% ($P < 0.001$ compared with insulin alone, $n = 6$; Fig. 1*B*). Treatment with 5 mM ASA and 10 μM TGZ during the final 24 h of the TNF-α treatment reversed the impairment in insulin-stimulated 2-DOG uptake by 28% ($P < 0.01$ compared with TNF-α alone, not significant compared with insulin alone; $n = 6$; Fig. 1*B*). The viability of the cells, as assessed by thiazolyl blue tetrazolium blue (MTT), remained unchanged with any of the treatments ($n = 3$, data not shown). Subsequent microarray analysis of vehicle (insulin sensitive)-, TNF-α (insulin resistant)-, and TNF-α plus ASA and TGZ (insulin resensitized)-treated samples ($n = 20$ per treatment group) identified 3,325 genes with evidence of differential expression in TNF-α-treated compared with vehicle-treated adipocytes (nominal $P < 0.01$). The TNF-α-induced change in expression of 1,022 of these genes was reversed after treatment with ASA and TGZ (nominal $P < 0.01$). This set of 1,022 genes was subjected to a Bayesian model selection procedure coupled with Bayesian model averaging to produce a five-gene GES that had a predictive power of 93% to discriminate between the insulin-resistant and insulin-resensitized states and, accordingly, was selected to be the TNF-α-based GES. These genes were identified as acyl-CoA synthetase 1 (ACS1), six transmembrane epithelial antigen of the prostate 4 (STEAP4), S-phase kinase associated protein 1A (Skp1a), pyruvate kinase muscle 2 (PKM2), and CD63 antigen (CD63) (see Table 2).

Microarray data revealed that expression of four of the five genes was increased by 1.4- to 2.7-fold after TNF-α treatment (STEAP4, PKM2, Skp1a, and CD63) while one gene (ACS1) had decreased expression by 60% relative to vehicle (Fig. 2*A*). TNF-α down- and upregulation of ACS1 and STEAP4 mRNA levels in adipocytes, respectively, have been reported previously (30, 48). To our knowledge, there have been no reports of direct TNF-α regulation of PKM2, Skp1a, and CD63 transcription in adipocytes. Each of the five genes was significantly

Table 2. *Identity of the 5 genes that comprise the TNF-α-based GES*

Gene Name	NCBI Reference No.	Proposed Function
ACS1/FACL2/palmitoyl-CoA ligase	NM_007981	Fatty acid transport and metabolism (39)
CD63 Antigen	NM_007653	Cell adhesion and motility (25)
STEAP4/TIARP/STAMP2	NM_054098	Iron/copper reductase; metabolic homeostasis regulator (33, 49)
Skp1a	NM_011543	Proubiquination; cell cycle regulator (34)
PKM2	NM_011099	Aerobic glycolysis; tumorigenesis (10)

different in level of gene expression between the vehicle- and TNF-α-treated states and between the TNF-α- and TNF-α plus ASA and TGZ-treated samples ($P < 0.005$, Fig. 2*A*). Expression of STEAP4, PKM2, and CD63 genes remained significantly different between vehicle and TNF-α plus ASA and TGZ treatments ($P < 0.002$), indicating only partial reversal of TNF-α effects by the insulin-sensitizing agents, while they fully restored ACS1 and Skp1a gene expression back to vehicle levels (see Fig. 2*A*). The change in expression for each gene was confirmed by qPCR (see Fig. 2*B*). Expression levels of all genes remained significantly different between vehicle and TNF-α treatments and between TNF-α and TNF-α plus ASA and TGZ treatments ($P < 0.05$).

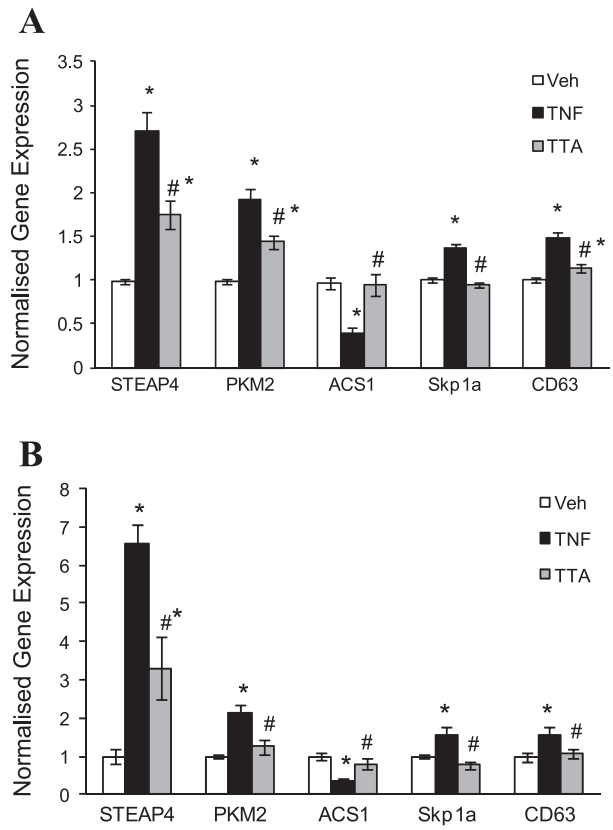

Fig. 2. Expression profiling of the TNF-α-based gene expression signature (GES). Microarray expression (*A*) and quantitative real-time PCR (qPCR) analysis (*B*) of the 5-gene GES in vehicle-treated (Veh), TNF-α-treated (TNF), and TNF-α + TGZ and ASA-treated (TTA) 3T3-L1 adipocytes are shown. Gene expression values are normalized to vehicle-treated cells (set at 1.0). Data are represented as means ± SE; $n = 20$ (*A*) or 5 (*B*) per treatment. Statistical analyses were performed with unpaired Student's *t*-test (*A*) or 1-way ANOVA with multiple testing correction with Tukey HSD (*B*). *$P < 0.05$ compared with Veh; #$P < 0.05$ compared with TNF.

Use of TNF-α-Based GES Screen to Identify Known and New Insulin Sensitizers

After the identification of the GES, we investigated the ability of the GES to identify agents with potential insulin-sensitizing properties. A compound library was screened in 3T3-L1 adipocytes with the TNF-α-based GES, in which the gene expression levels of the five GES genes were multiplexed and quantified with Sequenom's MALDI-TOF-based quantitative gene expression analysis system. The aim of the screen was to identify compounds that regulated the expression of the five-gene GES to resemble most closely the expression levels observed in the insulin-resensitized cells, as this is likely to indicate that these cells have restored insulin sensitivity. Of the 1,120 compounds screened, data from 852 compounds passed quality control. As detailed under EXPERIMENTAL PROCEDURES, a formula was developed to combine the expression levels of each of the five GES genes, the direction of change, and the relative contribution that each gene made to the predictive power of the GES into a single number, and this was termed the "GES score." Compounds were ranked highest to lowest based on each compound's GES score. A compound with a positive GES score may indicate similarity to the insulin-resensitized treatment group, and, conversely, a negative score may highlight a compound acting more like the insulin-resistant treatment group. To determine whether the GES screen enriched for compounds with insulin-sensitizing properties, the top ~10% ranked compounds from the screen were tested for their ability to affect GLUT4 translocation to the plasma membrane of 3T3-L1 adipocytes in the presence of submaximal (0.5 nM) insulin. We utilized the ELISA-based HA-tagged GLUT4 translocation assay for secondary screening of the compounds because this assay was amenable to a high-content screening platform, in contrast to the radioactive 2-DOG uptake assay. Cells were incubated with compounds at 10 μM for 24 h before the measurement of insulin-stimulated HA-tagged GLUT4 translocation. Controls in the HA-tagged GLUT4 translocation assay included 24-h incubation of 10 μM TGZ or 5 mM ASA alone. The percent increases over 0.5 nM insulin alone were as follows (means ± SE): 10 μM TGZ, 70 ± 20%; 5 mM ASA, 98 ± 17% ($P < 0.05$, $n = 8$). Of the 82 compounds tested, 57 compounds (~70%) were found to increase GLUT4 translocation to the plasma membrane in the presence of submaximal insulin by an average of 51 ± 5% over 0.5 nM insulin alone (see Table 3).

As an initial proof of concept and to assess plate-to-plate variation, a total of 30 compounds with a GES that most closely matched the insulin-resensitized cells within the same 96-well plate (14 plates in total, $n = 2$ or 3 compounds/plate) from the GES screen were subjected to 2-DOG uptake analysis in order to determine their potential insulin-sensitizing effects.

Table 3. *Validation of top 10% ranked compounds from TNF-α-based GES screen with GLUT4 translocation assay*

GES Score	Compound Name	Known Mechanism	GLUT4 Ratio
6.255	Indomethacin	NSAID	1.15
3.015	Alprenolol hydrochloride	β-Adrenergic antagonist	1.42
2.965	Nomegestrol acetate	Progestogens steroid	1.05
2.627	Mesalamine	NSAID	1.15
2.397	α-Santonin	NSAID	1.28
2.080	Hydrochlorothiazide	Carbonic anhydrase inhibitor	1.77
2.038	Bemegride	GABA antagonist	1.11
2.022	Articaine hydrochloride	Sodium channel blocker	0.86
1.916	Amiloride hydrochloride dihydrate	Sodium channel blocker	2.28
1.846	Meprylcaine hydrochloride	Serotonin antagonist	1.64
1.816	Tacrine hydrochloride hydrate	Cholinesterase inhibitor	0.44
1.765	Clidinium bromide	Cholinergic antagonist	1.11
1.674	Quinic acid	Sodium channel blocker	1.34
1.665	Viomycin sulfate	Antibiotic	1.13
1.640	Niacin	Vitamin	1.74
1.637	Ketanserin tartrate hydrate	Serotonin antagonist	1.87
1.597	Levodopa	Tyrosine aminotransferase inhibitor	2.43
1.592	Glutethimide, *para*-amino	Cytochrome *P*-450 inhibitor	1.18
1.589	Oxaprozin	NSAID	1.19
1.452	Myosmine	Cholinergic agonist	0.47
1.446	Sulfathiazole	Sulfamide antifolate	1.16
1.429	Nafcillin sodium salt monohydrate	β-Lactam	0.38
1.406	Glycopyrrolate	Cholinergic antagonist	1.28
1.389	Amprolium hydrochloride	Thiamine transport inhibitor	1.64
1.362	Natamycin	Aminoglycoside	1.34
1.350	Pivmecillinam hydrochloride	β-Lactam	1.40
1.331	Minaprine dihydrochloride	Cholinesterase inhibitor	1.60
1.330	(*R*)-propranolol hydrochloride	β-Adrenergic antagonist	1.24
1.300	Minocycline hydrochloride	Aminoglycoside	0.54
1.240	Tomatidine	Cholinesterase agonist	0.89
1.215	Benoxinate hydrochloride	Sodium channel blocker	2.04
1.203	Amrinone	Phosphodiesterase inhibitor	0.26
1.165	Tolnaftate	Antifungal	1.99
1.124	Acemetacin	NSAID	0.85
1.102	Epicatechin-(−)	Lipoxygenase inhibitor	0.76
1.083	Bisoprolol fumarate	β-Adrenergic antagonist	0.60
1.060	Promethazine hydrochloride	Cholinergic antagonist	0.90
1.040	Nizatidine	Histamine antagonist	0.85
1.037	Trifluoperazine dihydrochloride	Dopamine antagonist	0.65
1.022	Hexamethonium dibromide dihydrate	Cholinergic antagonist	1.86
0.996	Cefazolin sodium salt	β-Lactam	1.33
0.987	Amethopterin (*R*, *S*)	Folic acid antimetabolite	2.39
0.979	Oxethazaine	Sodium channel blocker	1.96
0.975	Benzamil hydrochloride	Sodium channel blocker	0.77
0.975	Avermectin B1	GABA antagonist	0.93
0.971	Esculin hydrate	Apoptosis inhibitor	1.61
0.966	Sertaconazole nitrate	Steroid synthesis inhibitor	1.40
0.956	Ronidazole	Antibiotic	1.17
0.944	Butirosin disulfate salt	Aminoglycoside	0.84
0.940	Hydroquinine hydrobromide hydrate	Phospholipid synthesis inhibitor	1.25
0.938	Mevalonic-D, L acid lactone	HMG-CoA reductase inhibitor	1.42
0.922	Cephalosporanic acid, 7-amino	β-Lactam	1.12
0.913	Urapidil hydrochloride	α-Adrenergic antagonist	2.28
0.913	Piperidolate hydrochloride	Cholinergic antagonist	1.71
0.908	Dubinidine	Alkaloid	1.13
0.907	Cefuroxime sodium salt	β-Lactam	0.86
0.902	Rauwolscine hydrochloride	α-Adrenergic antagonist	0.70
0.886	Benfotiamine	Vitamin	0.73
0.871	Pheniramine maleate	Histamine antagonist	1.66
0.869	Vitamin K2	Vitamin	1.32
0.866	Caffeic acid	Lipoxygenase inhibitor	1.65
0.860	Thioridazine hydrochloride	Calcium channel blocker	1.70
0.858	Suxibuzone	NSAID	0.90
0.856	Isoflupredone acetate	Glucocorticoid steroid	1.19
0.847	Dibucaine	Sodium channel blocker	1.44
0.846	Pyridoxine hydrochloride	Vitamin	1.40
0.835	Tremorine dihydrochloride	Cholinergic agonist	1.51
0.832	Mepenzolate bromide	Cholinergic antagonist	0.76

Continued

Table 3.—*Continued*

GES Score	Compound Name	Known Mechanism	GLUT4 Ratio
0.832	Enilconazole	Steroid synthesis inhibitor	0.47
0.829	(−)-Quinpirole hydrochloride	Dopamine antagonist	1.25
0.826	(*S*)-(−)-cycloserine	Antibiotic	1.12
0.823	Methazolamide	Carbonic anhydrase inhibitor	1.24
0.823	Cefsulodin sodium salt	β-Lactam	1.11
0.812	Bucladesine sodium salt	Adenylate cyclase modulator	0.96
0.806	Benzbromarone	Uric acid uptake inhibitor	1.52
0.786	Sulfabenzamide	Sulfamide antifolates	1.16
0.773	Prochlorperazine dimaleate	Cholinergic antagonist	1.73
0.772	Papaverine hydrochloride	Phosphodiesterase inhibitor	0.93
0.769	Raloxifene hydrochloride	Linear amine	1.41
0.766	Pyrimethamine	Folic acid antimetabolite	2.91
0.759	Penbutolol sulfate	β-Adrenergic agonist	1.17
0.741	Nortriptyline hydrochloride	Norepinephrine uptake inhibitor	1.29

Ranking by the GES score for each compound from the TNF-α-based GES screen is shown. GLUT4 ratio for each compound represents the fold change compared with 0.5 nM insulin alone (set at 1.0). Controls in the hemagglutinin HA-tagged GLUT4 translocation assay include 20-min incubation of 0 nM and 200 nM insulin alone and 24-h incubation of 10 μM troglitazone (TGZ) or 5 mM aspirin (acetylsalicylic acid, ASA). The fold changes compared with 0.5 nM insulin alone (set at 1.0) (i.e., GLUT4 ratio) were as follows (means ± SE): 0 nM insulin, 0.58 ± 0.04 ($P < 0.001$, $n = 30$); 200 nM insulin, 1.67 ± 0.14 ($P < 0.001$, $n = 30$); 10 μM TGZ, 1.70 ± 0.20 ($P < 0.05$, $n = 8$); and 5 mM ASA, 1.98 ± 0.17 ($P < 0.05$, $n = 8$). NSAID, nonsteroidal anti-inflammatory drug; GABA, γ-aminobutyric acid; HMG-CoA reductase, 3-hydroxy-3-methylglutaryl-CoA reductase.

3T3-L1 adipocytes were incubated for 24 h with each compound before performance of 2-DOG uptake assays in the presence or absence of submaximal insulin (0.5 nM for 30 min). Sixty-three percent of the 30 selected compounds from the GES screen increased insulin-stimulated glucose uptake by approximately twofold compared with 0.5 nM insulin alone ($P < 0.03$, $n = 2$) (Supplemental Fig. S1).[1]

The ranked compounds were broadly grouped into classes as determined by information on their molecular or therapeutic mechanism gained from database searches or by their structural features. Forty-two compound classes with at least five members were identified, and the data from the GES screen were represented as the mean GES score for each class and ranked (see Table 4). The mean GES score for the three control groups were as follows (means ± SE): vehicle (insulin sensitive), 1.758 ± 0.373; TNF-α plus TGZ and ASA (insulin resensitized), 0.043 ± 0.097; and TNF-α (insulin resistant), −0.318 ± 0.069. Furthermore, each group was statistically different from the others ($P < 0.001$, $n = 29$–57/group) (see Table 4). Apoptosis inhibitors, β-adrenergic antagonists, steroid synthesis inhibitors, nonsteroidal anti-inflammatory drugs (NSAIDs), vitamins, cholinesterase inhibitors, α-adrenergic antagonists, sodium channel blockers, β-lactams, and sulfamide antifolates had significantly increased GES scores compared with the TNF-α (insulin resistant) treatment group ($P < 0.05$, $n = 5$–38/family), suggesting that these families may contain compounds with potential insulin-sensitizing properties. Only glucocorticoids and β-adrenergic agonists scored significantly lower than the TNF-α treatment group ($P < 0.05$, $n = 13$–20/family). Similar to the TNF-α treatment group, the glucocorticoids, β-adrenergic agonists, progesterone steroids, and topoisomerase inhibitors scored significantly lower than the TNF-α plus TGZ and ASA (insulin resensitized) treatment group ($P < 0.05$, $n = 8$–20/family). Together, these data highlight the utility of the GES as a primary screen to identify compounds with insulin-sensitizing properties in vitro.

[1] Supplemental Material for this article is available online at the Journal website.

Use of TNF-α-Based GES to Characterize an Insulin-Resistant Subgroup of Individuals

We analyzed a global human gene expression data set to determine whether the in vitro-derived TNF-α-based GES had biological relevance in vivo. The profiling was undertaken in lymphocytes as part of the SAFHS (28), which mapped the expression levels of 47,289 transcripts in 1,240 individuals from 42 extended family pedigrees with Illumina bead-based technology (14). The frequency of diabetes in this population was 15.4%. The characteristics of the individuals were as follows (means ± SD): BMI, 29.3 ± 6.6 kg/m^2 ($n = 1,225$); fasting glucose, 100.6 ± 43.8 mg/dl ($n = 1,240$); and fasting insulin, 16.2 ± 19.1 U/ml ($n = 1,223$). We detected expression of the five genes comprising the TNF-α-based GES in the human lymphocyte data set. We then calculated a GES score as described above and looked for relationships between an individual's GES score and his/her phenotypic characteristics (see Fig. 3). After normalization for the effects of age, a higher degree of insulin resistance was observed in the individuals with a low GES score (most similar to the TNF-α-induced profile of the GES), as measured by their fasting plasma insulin levels ($\beta = -0.104$, $n = 1,035$; Fig. 3*B*) and HOMA_IR ($\beta = -0.092$, $n = 1,223$; Fig. 3*A*) ($P < 0.001$). On the basis of GES score, there was no statistically significant correlation with fasting glucose levels (see Fig. 3*C*), suggesting that the GES correlates predominantly with insulin resistance rather than diabetes. After the exclusion of individuals with diabetes, the correlation of GES score with insulin resistance remained equivalent for fasting plasma insulin levels ($\beta = -0.102$, $n = 1,025$) and HOMA_IR ($\beta = -0.106$, $n = 1,035$) ($P < 0.001$). No significant correlation was observed with any other clinical trait including BMI (Fig. 3*D*) or plasma levels of triglycerides, total cholesterol, and HDL (data not shown). This observation is consistent with the GES representing an insulin-resistant phenotype in this study population. Significantly, the same GES used above to screen for compounds with insulin-sensitizing properties has the ability to stratify individuals according to their insulin resistance status.

Table 4. *Ranking of compound families by TNF-α-based GES*

Drug Class	GES Score	*n*	*P* Value Compared with TNF	*P* Value Compared with TTA
Vehicle	1.758 ± 0.373	55	0.000	0.000
Apoptosis inhibitors	0.510 ± 0.172	5	0.003	0.020
β-Adrenergic antagonists	0.353 ± 0.215	17	0.000	0.274
Steroid synthesis inhibitors	0.323 ± 0.108	11	0.001	0.364
Norepinephrine release inhibitors	0.247 ± 0.181	5	0.065	1.000
NSAIDs	0.231 ± 0.222	38	0.009	1.000
Vitamins	0.186 ± 0.368	10	0.046	1.000
Sulfonylureas	0.168 ± 0.234	5	0.149	1.000
Cholinesterase inhibitors	0.157 ± 0.211	13	0.020	1.000
α-Adrenergic antagonists	0.153 ± 0.101	18	0.003	1.000
Sodium channel blockers	0.097 ± 0.174	29	0.018	1.000
β-Lactams	0.083 ± 0.155	26	0.016	1.000
GABA antagonists	0.067 ± 0.259	13	0.110	1.000
Sulfamide antifolates	0.052 ± 0.150	20	0.035	1.000
TTA	0.043 ± 0.097	29	0.000	1.000
Lipoxygenase inhibitors	0.018 ± 0.166	16	0.096	1.000
Dopamine antagonists	0.014 ± 0.264	11	0.243	1.000
Carbonic anhydrase inhibitors	0.007 ± 0.290	11	0.287	1.000
Antibiotics	−0.003 ± 0.213	13	0.211	1.000
Cholinergic agonists	−0.004 ± 0.139	19	0.090	1.000
Cholinergic antagonists	−0.028 ± 0.097	62	0.043	1.000
Calcium channel blockers	−0.061 ± 0.197	20	0.335	1.000
Estrogen steroids	−0.099 ± 0.184	8	0.813	1.000
Phosphodiesterase inhibitors	−0.126 ± 0.289	12	0.891	1.000
Na^+-K^+-ATPase inhibitors	−0.128 ± 0.252	5	1.000	1.000
Histamine antagonists	−0.141 ± 0.137	34	0.564	0.711
Serotonin antagonists	−0.150 ± 0.288	14	1.000	1.000
Dopamine agonists	−0.152 ± 0.173	7	1.000	1.000
Serotonin agonists	−0.152 ± 0.175	15	0.900	0.795
Linear amines	−0.163 ± 0.232	10	1.000	0.917
Topoisomerase inhibitors	−0.168 ± 0.208	9	1.000	0.011
ACE inhibitors	−0.177 ± 0.442	6	1.000	1.000
Aminoglycosides	−0.192 ± 0.187	26	1.000	0.545
Monoamine oxidase inhibitors	−0.199 ± 0.229	14	1.000	0.604
Nucleoside antimetabolites	−0.220 ± 0.179	13	1.000	0.442
Detergents	−0.262 ± 0.087	6	1.000	0.558
Na^+/Cl^- transport inhibitors	−0.307 ± 0.312	7	1.000	0.398
TNF	−0.318 ± 0.069	57	1.000	0.000
Contrast agents	−0.320 ± 0.144	11	1.000	0.151
α-Adrenergic agonists	−0.334 ± 0.212	13	1.000	0.137
Potassium channel blockers	−0.336 ± 0.514	6	1.000	0.464
Progesterone steroids	−0.483 ± 0.163	8	1.000	0.038
GABA agonists	−0.516 ± 0.322	5	1.000	0.099
β-Adrenergic agonists	−0.677 ± 0.237	13	0.003	0.020
Glucocorticoid steroids	−0.736 ± 0.193	20	0.025	0.000

GES score values are means ± SE. Ranking of the average GES score for each compound family is shown. The insulin-sensitive vehicle, insulin-resensitized TNF-α + TGZ and ASA (TTA), and insulin-resistant TNF-α alone (TNF) treatment groups are also included as controls. To determine which compound families had mean GES scores statistically different from the TNF and TTA treatment groups, the Kruskal-Wallis nonparametric test was used. *P* values were adjusted for multiple comparison testing with the Bonferroni correction. $P < 0.05$ was considered significant. ACE, angiotensin-converting enzyme.

DISCUSSION

In the present study, we have described the generation of a novel GES from a cell model to discriminate between "insulin-resistant" and "insulin-resensitized" states. The GES approach employed an unbiased selection of genes that were the most statistically different between insulin-resistant and insulin-resensitized cells. We have used these tools to establish the first compound library screening using a GES to identify insulin-sensitizing agents. This approach could be applicable to any other metabolic disease that can be modeled adequately in cell culture. In addition, the cell culture-derived GES was detected in the mRNA expression patterns of human lymphocytes, and individuals with more severe insulin resistance were identified on the basis of their GES score. These observations provide preliminary evidence that GES technology can potentially differentiate insulin resistance status in patients and be used to screen for compounds with insulin-sensitizing properties, providing the potential for development of personalized medicine for patients with type 2 diabetes.

Our results using the TNF-α-based GES to screen a compound library for agents able to reverse insulin resistance are promising. The GES was able to identify individual compounds and classes of compounds with documented in vitro and in vivo insulin-sensitizing effects that scored similarly to the insulin-resensitized GES. In other words, the compounds were able to mimic the GES gene expression changes induced by ASA and TGZ. These classes of compounds include the NSAIDs, β-adrenergic antagonists, steroid synthesis inhibitors,

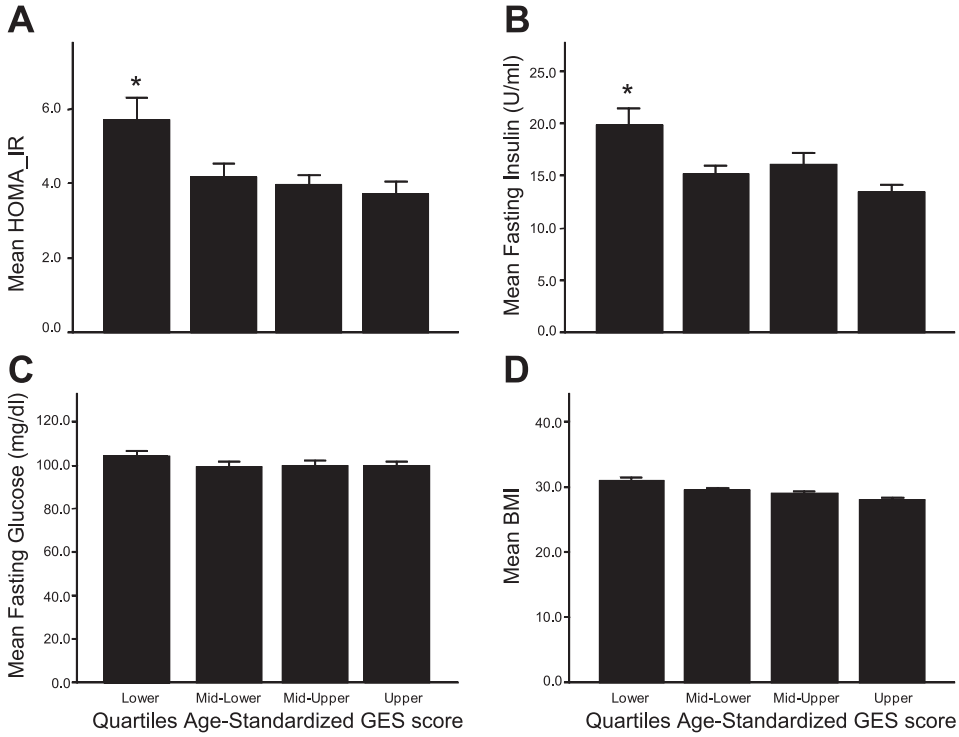

Fig. 3. TNF-α-based GES-characterized individuals according to their level of insulin resistance. Each individual's GES score was utilized to look for a relationship with the clinical traits available in the San Antonio Family Heart Study (SAFHS) data set with Pearson's correlation. *A*: the direction of the correlation between quartiles of the age-standardized GES score and measures of insulin resistance (HOMA_IR) is shown. *B* and *C*: the relationship with levels of fasting plasma insulin (*B*) and glucose (*C*) is shown; observe that the correlation with HOMA_IR is based primarily on the insulin component. *D*: no significant correlation was observed with body mass index (BMI), although a trend was noted. Data are represented as means ± SE. *P* values were corrected for multiple comparison with a conservative Bonferroni correction. $*P < 0.001$ compared with the other 3 quartiles.

vitamins, cholinesterase inhibitors, and sodium channel blockers (23, 40, 43, 44, 50, 51). For example, higher-than-conventional doses of NSAIDs have been shown to lower plasma glucose levels in individuals with type 2 diabetes (6, 31). The mechanism(s) of the glucose-lowering action of these compounds are varied and include inhibition of cyclooxygenase (COX) activity and PGE_2 production (indomethacin with a GES score of 6.255; ibuprofen, 0.476) (17, 38), free radical scavenger and antioxidant (mesalamine, 2.627) (5), inhibition of NF-κB activation (niflumic acid, 0.614) (3, 4) and regulation of peroxisome proliferator-activated receptors (PPARs) (indomethacin; dicoflenac, 0.347) (1, 24). The beta-blocker propranolol (1.330) has been reported to ameliorate TNF-α-induced insulin resistance in rats (23). Likewise, further investigation of the compounds comprising the class of sodium channel blockers class revealed that many of them are known to affect glucose and lipid metabolism, including quinic acid (1.673), procaine (0.312), and disopyramide (0.126) (8, 16, 19, 44). The screen also identified compounds from families such as the β-lactams, sulfamide antifolates, and carbonic anhydrase inhibitors that have not been characterized in terms of insulin-sensitizing actions. Conversely, families that scored poorly (similar to the insulin-resistant GES), such as glucocorticoids and β-adrenergic agonists, have previously been shown to induce insulin resistance both in vitro and in vivo, such as prednisolone (−0.291), corticosterone (−2.722), methyl prednisolone (−1.534), isoproterenol (−0.056), fenoterol (−1.042), and terbutaline (−2.425) (18, 21, 22, 35–37, 45). Further studies are now under way to confirm whether the novel compounds and/or classes that scored similarly to the insulin-resensitized GES have the ability to act as insulin-sensitizing agents in vivo.

Gene expression profiling is being utilized increasingly in human lymphocytes to help characterize the pathogenic states of individuals. Such an application is appealing for several reasons. It is relatively noninvasive and has the potential to identify early stages of disease progression. GESs derived from peripheral $CD4^+$ T cells were used to discriminate between individuals with acute and chronic hepatitis B infection (46) and as a detection marker for early stages of fibrosarcomas (26). GES profiling in lymphocytes has also been employed as a molecular marker to differentiate between Alzheimer's disease patients and unaffected individuals (13). This particular study demonstrated that multiple diseases, regardless of their etiology, will activate overlapping pathways such as inflammation, oxidative stress, and cholesterol biosynthesis, which can be reflected in the gene expression profile of lymphocytes and macrophages, making these cell populations useful to monitor disease onset and progression (13). Our study extends these important applications by demonstrating the utility of the first GES to differentiate between levels of insulin resistance in a human population using minimally invasive technology. The critical point demonstrated in our study is that the same GES used to subtype the patients was used to screen for insulin-sensitizing compounds that could be targeted to that subtype of insulin resistance. The outcome may provide a means for the development of therapeutic intervention that is specific to the disease subtype.

Despite the fact that the GES genes are identified statistically and irrespective of their physiological functions (if known), we have data to suggest that there is potential for these genes to play a role in the development of insulin resistance. Since very little was known about STEAP4 at the time and its gene expression levels were induced approximately sevenfold by TNF-α (Fig. 2*B*), we used small hairpin RNA (shRNA) technology to effectively silence endogenous STEAP4 mRNA levels in 3T3-L1 adipocytes by ~80% ($P < 0.005$, $n = 6$ compared with jumble shRNA-infected adipocytes) and found

that insulin-stimulated glucose transport was impaired in the STEAP4 shRNA-infected cells by ~25% ($P < 0.05$, $n = 4$) (Supplemental Fig. S2). We hypothesize that this particular gene was increased in response to TNF-α in order to protect the cells against the TNF-α insult. A study was published by Hotamisligil's laboratory (49) just as we had established our preliminary findings, demonstrating in vitro and in vivo that STEAP4 is protective against inflammatory processes and metabolic deregulation. The finding with STEAP4 highlights an additional unforeseen utility of the TNF-α-based GES approach: the potential identification of novel diabetes candidates.

In the present study, we combined a cellular model with clinical investigation and a high-content screen to tackle the complex, heterogeneous nature of insulin resistance. Presently, there are significant challenges to finding effective therapies for the long-term management of type 2 diabetes. This study offers proof of concept that the GES approach can be used for the identification of optimized treatments in a multitude of diseases with multifactorial etiology. The ability to both characterize the heterogeneity of insulin resistance and specifically target treatment of individuals according to their subtype(s) of insulin resistance at clinical presentation has the potential to promote the development of optimized medical treatments (i.e., personalizing medicine) for patients with type 2 diabetes.

ACKNOWLEDGMENTS

We are very grateful to Dr. Janette Tenne-Brown, Sharon Jones, and Reuben Klein for technical assistance and to Dr. Nicole Stupka, Dr. Sean McGee, Prof. Andy Sinclair, Prof. Mike Cawthorne, and Prof. Steve Shoelson for thoughtful comments on the manuscript.

Present addresses: V. C. Foletta, School of Exercise and Nutrition Sciences, Deakin University, Melbourne, VIC 3125, Australia; D. H. Segal, Chemical Biology Division, Walter and Eliza Hall Institute of Medical Research, Melbourne, VIC 3052, Australia; K. A. Shields, Defence Science and Technology Organisation, Melbourne, VIC 3000, Australia; S. Wanyonyi, Institute of Technology & Research Innovation, Deakin University, Geelong, VIC 3217, Australia; G. Krippner, Medicinal Chemistry, Baker IDI Heart and Diabetes Institute, Melbourne, VIC 3004, Australia.

DISCLOSURES

Author contributions: N. Konstantopoulos, V. C. Foletta, G. R. Collier, and K. R. Walder designed the research study; N. Konstantopoulos, C. Swinton, S. Wanyonyi, T. Connor, and R. P. Fahey performed the cellular studies, microarrays, GES validation, high-content compound screen, secondary GLUT4 screen, proof-of-concept 2-DOG uptake screen, and subsequent data analysis; A. Sanigorski, T. D. Dyer, and J. Blangero performed the bioinformatics to identify the GES; K. A. Shields and J. B. Jowett performed the MassARRAY and subsequent data analysis; J. B. Jowett, J. E. Curran, and J. Blangero performed the human data set analysis; N. Konstantopoulos, A. Sanigorski, J. B. Jowett, and G. Krippner performed the GES-based screen data analysis; N. Konstantopoulos, V. C. Foletta, and R. A. Watt performed the STEAP4 study; D. E. James contributed the GLUT4 screen analytic tools; K. R. Walder, D. E. James, K. Windmill, and D. H. Segal contributed critical intellectual content to drafting of the paper; N. Konstantopoulos and V. C. Foletta wrote the paper.

This work was supported by ChemGenex Pharmaceuticals Ltd and Verva Pharmaceuticals Ltd, Australia.

The authors declare that G. Krippner is a current employee of Verva Pharmaceuticals. G. R. Collier is a current employee and K. R. Walder and D. E. James are past employees of ChemGenex Pharmaceuticals. D. E. James and J. Blangero were scientific advisors to ChemGenex Pharmaceuticals. The authors disclose that K. R. Walder, J. B. Jowett, J. Blangero, and D. E. James received research grants from Verva Pharmaceuticals or ChemGenex Pharmaceuticals.

REFERENCES

1. **Adamson DJ, Frew D, Tatoud R, Wolf CR, Palmer CNA.** Diclofenac antagonizes peroxisome proliferator-activated receptor-γ signaling. *Mol Pharmacol* 61: 7–12, 2002.
2. **Alizadeh AA, Eisen MB, Davis RE, Ma C, Lossos IS, Rosenwald A, Boldrick JC, Sabet H, Tran T, Yu X, Powell JI, Yang L, Marti GE, Moore T, Hudson J Jr, Lu L, Lewis DB, Tibshirani R, Sherlock G, Chan WC, Greiner TC, Weisenburger DD, Armitage JO, Warnke R, Levy R, Wilson W, Grever MR, Byrd JC, Botstein D, Brown PO, Staudt LM.** Distinct types of diffuse large B-cell lymphoma identified by gene expression profiling. *Nature* 403: 503–511, 2000.
3. **Alpert E, Gruzman A, Lardi-Studler B, Cohen G, Reich R, Sasson S.** Cyclooxygenase-2 (PTGS2) inhibitors augment the rate of hexose transport in L6 myotubes in an insulin- and AMPKα-independent manner. *Diabetologia* 49: 562–570, 2006.
4. **Alpert E, Gruzman A, Tennenbaum T, Sasson S.** Selective cyclooxygenase-2 inhibitors stimulate glucose transport in L6 myotubes in a protein kinase Cdelta-dependent manner. *Biochem Pharmacol* 73: 368–377, 2007.
5. **Ancha H, Kurella R, McKimmey C, Lightfoot S, Harty R.** Effects of *N*-acetylcysteine plus mesalamine on prostaglandin synthesis and nitric oxide generation in TNBS-induced colitis in rats. *Dig Dis Sci* 54: 758–766, 2009.
6. **Baron SH.** Salicylates as hypoglycemic agents. *Diabetes Care* 5: 64–71, 1982.
7. **Blangero J, Goring HH, Kent JW Jr, Williams JT, Peterson CP, Almasy L, Dyer TD.** Quantitative trait nucleotide analysis using Bayesian model selection. *Hum Biol* 77: 541–559, 2005.
8. **Boden WE, Moss AJ, Oakes D.** Hypolipidemic effect of type Ia antiarrhythmic agents in postinfarction patients. *Circulation* 85: 2039–2044, 1992.
9. **Carey KA, Segal D, Klein R, Sanigorski A, Walder K, Collier GR, Cameron-Smith D.** Identification of novel genes expressed during rhabdomyosarcoma differentiation using cDNA microarrays. *Pathol Int* 56: 246–255, 2006.
10. **Christofk HR, Vander Heiden MG, Wu N, Asara JM, Cantley LC.** Pyruvate kinase M2 is a phosphotyrosine-binding protein. *Nature* 452: 181–186, 2008.
11. **Cooper CS, Campbell C, Jhavar S.** Mechanisms of disease: biomarkers and molecular targets from microarray gene expression studies in prostate cancer. *Nat Clin Pract Urol* 4: 677–687, 2007.
12. **Cullinan A, Cantor C.** Sequenom, Inc. *Pharmacogenomics* 9: 1211–1215, 2008.
13. **Fehlbaum-Beurdeley P, Jarrige-Le Prado AC, Pallares D, Carriere J, Guihal C, Soucaille C, Rouet F, Drouin D, Sol O, Jordan H, Wu D, Lei L, Einstein R, Schweighoffer F, Bracco L.** Toward an Alzheimer's disease diagnosis via high-resolution blood gene expression. *Alzheimers Dement* 6: 25–38, 2010.
14. **Goring HHH, Curran JE, Johnson MP, Dyer TD, Charlesworth J, Cole SA, Jowett JBM, Abraham LJ, Rainwater DL, Comuzzie AG, Mahaney MC, Almasy L, MacCluer JW, Kissebah AH, Collier GR, Moses EK, Blangero J.** Discovery of expression QTLs using large-scale transcriptional profiling in human lymphocytes. *Nat Genet* 39: 1208–1216, 2007.
15. **Govers R, Coster AC, James DE.** Insulin increases cell surface GLUT4 levels by dose dependently discharging GLUT4 into a cell surface recycling pathway. *Mol Cell Biol* 24: 6456–6466, 2004.
16. **Hope-Gill H, Vydelingum N, Kissebah AH, Tulloch BR, Fraser TR.** Simulation and enhancement of the adipose tissue insulin response by procaine hydrochloride: evidence for a role of calcium in insulin action. *Horm Metab Res* 6: 457–463, 1974.
17. **Jaradat MS, Wongsud B, Phornchirasilp S, Rangwala SM, Shams G, Sutton M, Romstedt KJ, Noonan DJ, Feller DR.** Activation of peroxisome proliferator-activated receptor isoforms and inhibition of prostaglandin H_2 synthases by ibuprofen, naproxen, and indomethacin. *Biochem Pharmacol* 62: 1587–1595, 2001.
18. **Kajita K, Ishizuka T, Miura A, Kanoh Y, Ishizawa M, Kimura M, Muto N, Yasuda K.** Glucocorticoid-induced insulin resistance associates with activation of protein kinase C isoforms. *Cell Signal* 13: 169–175, 2001.
19. **Kojima Y, Yoshikawa Y, Ueda E, Ueda R, Yamamoto S, Kumekawa K, Yanagihara N, Sakurai H.** Insulinomimetic zinc(II) complexes with natural products: in vitro evaluation and blood glucose lowering effect in

KK-Ay mice with type 2 diabetes mellitus. *Chem Pharm Bull (Tokyo)* 51: 1006–1008, 2003.
20. **Konstantopoulos N, Marcuccio S, Kyi S, Stoichevska V, Castelli LA, Ward CW, Macaulay SL.** A purine analog kinase inhibitor, calcium/calmodulin-dependent protein kinase II inhibitor 59, reveals a role for calcium/calmodulin-dependent protein kinase II in insulin-stimulated glucose transport. *Endocrinology* 148: 374–385, 2007.
21. **Kralisch S, Klein J, Lossner U, Bluher M, Paschke R, Stumvoll M, Fasshauer M.** Isoproterenol stimulates monocyte chemoattractant protein-1 expression and secretion in 3T3-L1 adipocytes. *Regul Pept* 135: 12–16, 2006.
22. **Kralisch S, Klein J, Lossner U, Bluher M, Paschke R, Stumvoll M, Fasshauer M.** Isoproterenol, TNFalpha, and insulin downregulate adipose triglyceride lipase in 3T3-L1 adipocytes. *Mol Cell Endocrinol* 240: 43–49, 2005.
23. **Lang CH.** Beta-adrenergic blockade attenuates insulin resistance induced by tumor necrosis factor. *Am J Physiol Regul Integr Comp Physiol* 264: R984–R991, 1993.
24. **Lehmann JM, Lenhard JM, Oliver BB, Ringold GM, Kliewer SA.** Peroxisome proliferator-activated receptors α and γ are activated by indomethacin and other non-steroidal anti-inflammatory drugs. *J Biol Chem* 272: 3406–3410, 1997.
25. **Maecker H, Todd S, Levy S.** The tetraspanin superfamily: molecular facilitators. *FASEB J* 11: 428–442, 1997.
26. **Marques MMC, Junta CM, Zarate-Blades CR, Sakamoto-Hojo ET, Donadi EA, Passos GAS.** Transcriptional response of peripheral lymphocytes to early fibrosarcoma: a model system for cancer detection based on hybridization signatures. *Exp Biol Med* 234: 802–812, 2009.
27. **Miles PD, Romeo OM, Higo K, Cohen A, Rafaat K, Olefsky JM.** TNF-alpha-induced insulin resistance in vivo and its prevention by troglitazone. *Diabetes* 46: 1678–1683, 1997.
28. **Mitchell BD, Kammerer CM, Blangero J, Mahaney MC, Rainwater DL, Dyke B, Hixson JE, Henkel RD, Sharp RM, Comuzzie AG, VandeBerg JL, Stern MP, MacCluer JW.** Genetic and environmental contributions to cardiovascular risk factors in Mexican Americans: the San Antonio Family Heart Study. *Circulation* 94: 2159–2170, 1996.
29. **Mlinar B, Marc J, Janez A, Pfeifer M.** Molecular mechanisms of insulin resistance and associated diseases. *Clin Chim Acta* 375: 20–35, 2007.
30. **Moldes M, Lasnier F, Gauthereau X, Klein C, Pairault J, Feve B, Chambaut-Guerin AM.** Tumor necrosis factor-alpha-induced adipose-related protein (TIARP), a cell-surface protein that is highly induced by tumor necrosis factor-alpha and adipose conversion. *J Biol Chem* 276: 33938–33946, 2001.
31. **Mork NL, Robertson RP.** Effects of nonsteroidal antiinflammatory drugs in conventional dosage on glucose homeostasis in patients with diabetes. *West J Med* 139: 46–49, 1983.
32. **Nuyten DS, Hastie T, Chi JT, Chang HY, van de Vijver MJ.** Combining biological gene expression signatures in predicting outcome in breast cancer: an alternative to supervised classification. *Eur J Cancer* 44: 2319–2329, 2008.
33. **Ohgami RS, Campagna DR, McDonald A, Fleming MD.** The Steap proteins are metalloreductases. *Blood* 108: 1388–1394, 2006.
34. **Peters JM.** SCF and APC: the Yin and Yang of cell cycle regulated proteolysis. *Curr Opin Cell Biol* 10: 759–768, 1998.
35. **Peterson A, Peterson K, Tongen S, Guzman M, Corbett V, Langer O, Mazze R.** Glucose intolerance as a consequence of oral terbutaline treatment for preterm labor. *J Fam Pract* 36: 25–31, 1993.
36. **Rizza R, Mandarino L, Gerich J.** Cortisol-induced insulin resistance in man: impaired suppression of glucose production and stimulation of glucose utilization due to a postreceptor defect of insulin action. *J Clin Endocrinol Metab* 54: 131–138, 1982.
37. **Rooney DP, Neely RD, Cullen C, Ennis CN, Sheridan B, Atkinson AB, Trimble ER, Bell PM.** The effect of cortisol on glucose/glucose-6-phosphate cycle activity and insulin action. *J Clin Endocrinol Metab* 77: 1180–1183, 1993.
38. **Sandra A, Marshall SJ.** Arachidonic acid inhibition of insulin action and phosphoinositide turnover in fat cells. *Mol Cell Endocrinol* 45: 105–111, 1986.
39. **Soupene E, Fyrst H, Kuypers FA.** Mammalian acyl-CoA:lysophosphatidylcholine acyltransferase enzymes. *Proc Natl Acad Sci USA* 105: 88–93, 2008.
40. **Stankiewicz M, Norman R.** Diagnosis and management of polycystic ovary syndrome: a practical guide. *Drugs* 66: 903–912, 2006.
41. **Stegmaier K, Ross KN, Colavito SA, O'Malley S, Stockwell BR, Golub TR.** Gene expression-based high-throughput screening (GE-HTS) and application to leukemia differentiation. *Nat Genet* 36: 257–263, 2004.
42. **Stegmaier K, Wong JS, Ross KN, Chow KT, Peck D, Wright RD, Lessnick SL, Kung AL, Golub TR.** Signature-based small molecule screening identifies cytosine arabinoside as an EWS/FLI modulator in Ewing sarcoma. *PLoS Med* 4: e122, 2007.
43. **Stirban A, Negrean M, Stratmann B, Gawlowski T, Horstmann T, Gotting C, Kleesiek K, Mueller-Roesel M, Koschinsky T, Uribarri J, Vlassara H, Tschoepe D.** Benfotiamine prevents macro- and microvascular endothelial dysfunction and oxidative stress following a meal rich in advanced glycation end products in individuals with type 2 diabetes. *Diabetes Care* 29: 2064–2071, 2006.
44. **Taketa K, Yamamoto Y.** Hypoglycemic effect of disopyramide in a case of diabetes mellitus under insulin treatment. *Acta Med Okayama* 34: 289–292, 1980.
45. **Tappy L.** Metabolic effects of glucocorticoids: the unfinished story. *Eur J Clin Invest* 29: 814–815, 1999.
46. **Trehanpati N, Geffers R, Sukriti Hissar S, Riese P, Toepfer T, Buer J, Kumar M, Guzman CA, Sarin SK.** Gene expression signatures of peripheral CD4+ T cells clearly discriminate between patients with acute and chronic hepatitis B infection. *Hepatology* 49: 781–790, 2009.
47. **van de Vijver MJ, He YD, van't Veer LJ, Dai H, Hart AA, Voskuil DW, Schreiber GJ, Peterse JL, Roberts C, Marton MJ, Parrish M, Atsma D, Witteveen A, Glas A, Delahaye L, van der Velde T, Bartelink H, Rodenhuis S, Rutgers ET, Friend SH, Bernards R.** A gene-expression signature as a predictor of survival in breast cancer. *N Engl J Med* 347: 1999–2009, 2002.
48. **Weiner FR, Smith PJ, Wertheimer S, Rubin CS.** Regulation of gene expression by insulin and tumor necrosis factor alpha in 3T3-L1 cells. Modulation of the transcription of genes encoding acyl-CoA synthetase and stearoyl-CoA desaturase-1. *J Biol Chem* 266: 23525–23528, 1991.
49. **Wellen KE, Fucho R, Gregor MF, Furuhashi M, Morgan C, Lindstad T, Vaillancourt E, Gorgun CZ, Saatcioglu F, Hotamisligil GS.** Coordinated regulation of nutrient and inflammatory responses by STAMP2 is essential for metabolic homeostasis. *Cell* 129: 537–548, 2007.
50. **Yin J, Xing H, Ye J.** Efficacy of berberine in patients with type 2 diabetes mellitus. *Metabolism* 57: 712–717, 2008.
51. **Yuan M, Konstantopoulos N, Lee J, Hansen L, Li ZW, Karin M, Shoelson SE.** Reversal of obesity- and diet-induced insulin resistance with salicylates or targeted disruption of Ikkbeta. *Science* 293: 1673–1677, 2001.